JOURNAL OF MATERIALS SCIENCE 35 (2000) 547–554

Mechanical buckling instability of thin coatings deposited on soft polymer substrates

A. L. VOLYNSKII
Chemical Department, Moscow State University, 119890 Moscow, Russia

S. BAZHENOV*
Institute of Chemical Physics, Kosygin Street 4, 117977 Moscow, Russia

O. V. LEBEDEVA, N. F. BAKEEV
Institute of Synthetic Polymer Materials, Profsoyuznaya Street 70, 117393 Moscow, Russia

Deformation of rubber and poly(ethylene terephthalate) coated with a platinum or a gold film was studied. The thickness of the coating film was approximately ten nanometers. The polymer substrates were 10^4 to 10^5-fold softer than the coating. Folding of the coating leading to the appearance of a wave-like pattern on an originally smooth surface was observed both in tension and after shrinkage. In tension the wave crests are oriented along the elongation direction. After shrinkage the wave crests are perpendicular to the shrinkage direction. For rubber substrates, the appearance of the wave is explained by a mechanical buckling instability of the coating under compressive force. The length of the surface wave depends on the thickness of the coating layer and the rigidity of the polymer substrate. In addition to folding, regular fragmentation of the coating film on long and comparatively narrow bands is observed. The cracks are perpendicular to the wave crests both in tension and after shrinkage.

1. Introduction

Mechanical behavior of polymers coated with a thin (nanometers in thickness) rigid film attracts growing interest of researchers. The appearance of an irregular two-dimensional network of cracks in copper and chromium coatings on a polyimide substrate under uniaxial tensile load was reported [1]. Similar irregular cracking was observed when a coating was under a biaxial tensile load [2, 3]. In contrast, regular cracking of Pt and Au coatings on long and comparatively narrow bands was observed when poly(ethylene terephthalate) (PET) and rubber substrates were uniaxially elongated to 50–200% strain [4–6]. Similar behavior was observed in PET coated by SiO_2 film at low strains when the response of the substrate was elastic [7, 8].

In addition to cracking of a coating, the wave-like pattern appeared on an originally smooth surface during axial tension of rubber coated by Pt or Au film [9, 10]. Rubber was $\approx 10^5$-fold softer than the coating, and formation of the surface wave was explained by mechanical buckling instability of the coating under compressive force.

The appearance of a regular pattern on an originally smooth surface was observed previously in a swelling polymer gel immersed in a liquid [11, 12]. This phenomenon was explained by a mechanical buckling instability of the soft surface gel layer under growing compressional stress. Periodic buckling of a glass fiber embedded in an epoxy resin under compressive force has been observed [13].

Originally the problem of mechanical buckling instability of a rod under compressive force was introduced by Euler [14]. The buckled rod looks like a sector of a circle. According to Winkler, the shape of the rod is different if it lays on an elastic foundation, the stress in which is proportional to the deflection of the rod [15, 16]. The shape of the buckled rod on an elastic foundation is periodic and wave-like. Half-space was considered as an elastic foundation by Biot and the "modulus of foundation" was determined [17]. Buckling instability of an elastic beam embedded in an elastic medium was also considered by Biot [18, 19].

2. Experimental

Commercial films of amorphous unoriented poly(ethylene terephthalate), synthetic isoprene rubber, and natural rubber were used as polymer substrates. The thickness of the PET film was 100 μm. Natural rubber was cross-linked at 150 °C by 4 weight parts of dicumyl peroxide per 100 weight parts of raw rubber. Isoprene rubber was cross-linked at 150 °C by 1.5 weight parts of dicumyl peroxide per 100 weight parts of the rubber. The thickness of natural and isoprene rubber layers was 500 μm. Samples, dumbbell in shape, were cut

* Author to whom all correspondence should be addressed.

from the polymer layer. The gauge size of samples was 6×22 mm.

Ion sputtering deposition was used to coat specimens with a thin (≈10 nm in thickness) platinum or gold layer. This method is used to provide electric conductivity of samples for SEM studies. Then, the specimen was elongated with an Instron 1122 testing machine. Coated rubber was elongated in special hand-operated clamps. After elongation, the cracked metal surface was coated by the second platinum layer and studied by a Hitachi S-520 scanning electron microscope (SEM).

To study shrinkage, uncoated natural rubber was elongated, coated by a platinum film in the elongated state, and released from the grips. After unloading, the rubber shrank to its initial size (the coating was approximately 20,000-fold thinner than the rubber substrate).

The temperature dependence of an elasticity modulus was studied by dynamic test with a Rheometrics Solids Analyzer at 31 Hz frequency and 2 K/min heating rate.

The thickness of the platinum layer was changed by variation of time of deposition. To measure the thickness of the coating, Pt was deposited on a smooth glass surface. The coating was scratched, and the depth of the scratch was measured by a Nanoscope atomic-force microscope (Digital Instruments, Santa Barbara, USA) in contact force regime. The probe-sample interaction force was maintained constant and equal to 10^{-9} N. The coating thickness was proportional to time of deposition. The coefficient of proportionality was found, thus allowing determination of the thickness of the deposited platinum layer.

3. Results

3.1. Elongation

Fig. 1 shows an SEM micrograph of PET substrate coated with a gold film, and elongated to 300% strain at 85 °C. The arrow shows the direction of elongation. The white bands, perpendicular to the elongation direction, are gold bands. The width of the gold bands varies. The dark bands show PET substrate made visible due to opening of cracks in the coating. The coating is folded so that the surface is wavy, and the wave crests are parallel to the tension direction. The amplitude of the waves is almost constant over the entire area of the photograph. In the center of the PET bands, lines showing the initial position of cracks in the coating may be noticed. These lines are analogous to mid-ribs in crazes appearing under tensile load in polymers. The opposite surface of the sample, which was not coated by gold film, is plane.

Fig. 2 shows an SEM micrograph of a natural rubber coated by a gold film and elongated to 50% strain at room temperature. The sample was studied in elongated state. The surface pattern is similar to that in Fig. 1. Both the wave and cracks in the coating are observed. The opening of cracks is less than in Fig. 1 due to lower elongation of the sample. "Mid-ribs" in the center of the rubber bands are not observed. With the rubber substrate the wave disappeared after unloading.

3.2. Onset of folding

Onset of folding in rubber/Pt was studied visually. A specimen was elongated slowly with a test machine.

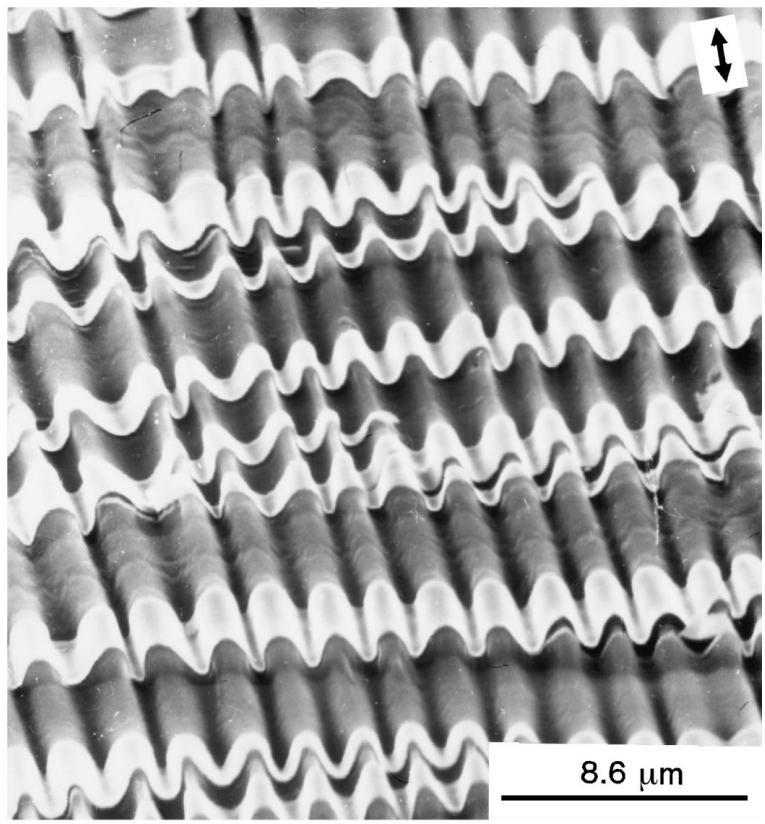

Figure 1 SEM micrograph of a poly(ethylene terephthalate) substrate coated with a gold film, and elongated to 300% at 85 °C. The thickness of the gold film is ≈10 nm.

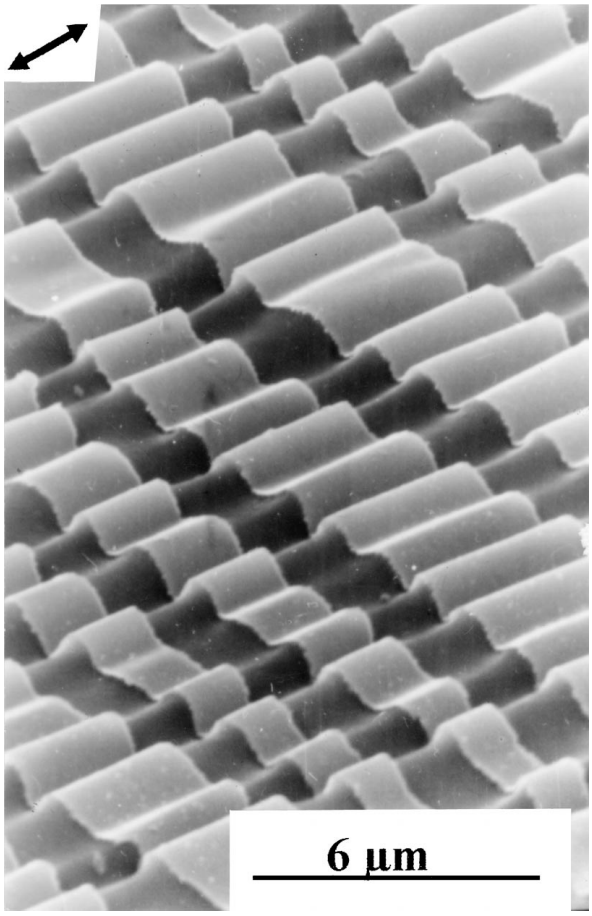

Figure 2 SEM micrograph of a natural rubber/Au elongated to 50% strain at room temperature.

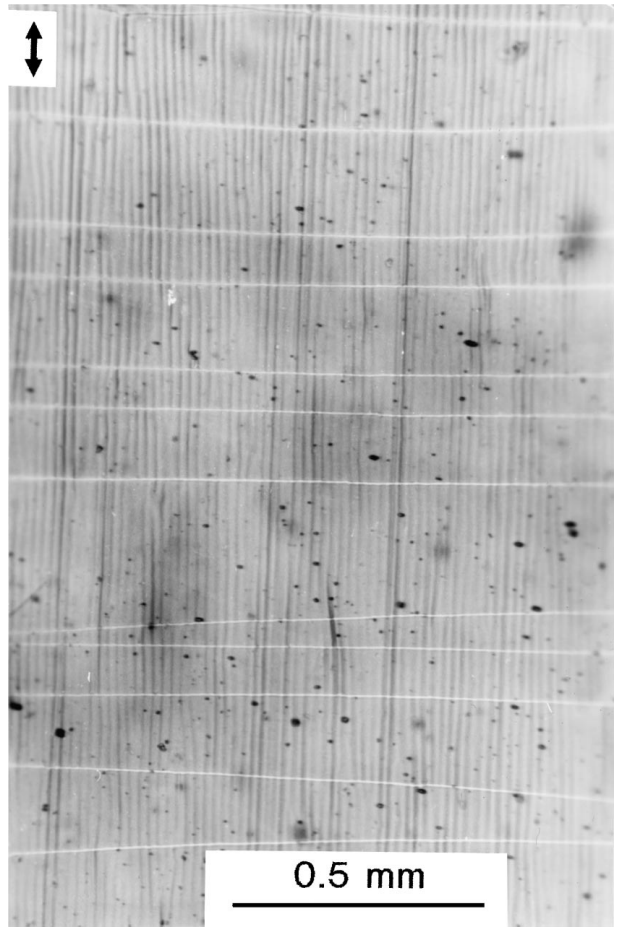

Figure 3 Optical micrograph of a natural rubber/Pt elongated to 2% strain at room temperature.

Light of a lamp was directed on the coated surface under the angle of 20–30°. Suddenly the sample in reflected light became colored. The colored region appeared near an edge of the sample and quickly spread over the entire surface of the sample. The time of spreading of the colored region was less then one second. Optical microscopy showed that before the critical moment the coating was smooth. After this moment, the coating was regularly folded. The example is presented in Fig. 3 which shows the surface of natural rubber/Pt at 2% strain, right after folding. Thus, the coating occasionally folds at some location, possibly near a defect, and the folded region quickly spreads over the entire specimen. With the rubber substrate, the folding of the coating is a critical phenomenon. The folding disappears after unloading.

The folding of the coating is explained by compression of the coating in the lateral direction. However, compression of the coating at axial elongation is not evident. The volume of the elongated rubber remains constant, and the Poisson's coefficient is 0.5. The Poisson's coefficient of Pt is lower, 0.36 [20]. In tension lateral contraction of the coating would be lower if it were not adhered to the rubber. The coating is thin, and its lateral contraction is determined by the rubber. As a result, the coating is compressed in the lateral direction. We assume that compression leads to mechanical buckling instability and folding of the coating. To verify this assumption, behavior of the coated rubber was studied during shrinkage.

3.3. Shrinkage

The rubber for these tests was coated in the elongated state. When the sample was released from the grips, the rubber shrank and compressed the coating. Fig. 4 shows an SEM micrograph of an isoprene rubber/Pt after shrinkage in the horizontal direction. The surface pattern in Fig. 4 is similar to that in Fig. 1. The wave crests are perpendicular to the shrinkage direction.

In tension, folding of the coating is caused by lateral contraction of the rubber. Similarly, during shrinkage, cracking of the coating in Fig. 4 is caused by lateral elongation of the rubber. The cracks are perpendicular to the direction of lateral tension as illustrated schematically by Fig. 5. As a result, the cracks are parallel to the shrinkage direction. The mechanism of folding of the coating under compressive force is illustrated schematically by Fig. 6.

3.4. Effect of strain

The surface wave appears at some initial strain, and further deformation changes the wavelength. Fig. 7 shows the length of the wave which appeared after shrinkage of an isoprene rubber plotted against the initial tensile strain of the rubber. The wavelength, λ, reduces as strain, ε, increases. Fig. 8 shows that in tension the wavelength also reduces with an increase in tensile strain ε. It was assumed that reduction of the wavelength λ is caused by the change of the specimen size under deformation.

Figure 4 SEM micrograph of isoprene rubber, elongated without coating to 50%, coated with Pt film and released from grips.

The change of size after shrinkage is characterized by the ratio $R = L_2/L_1 = 1/(1 + \varepsilon)$, (Fig. 7), where L_2 is the length of the specimen after shrinkage, and L_1 is its length before shrinkage. During tension, the change of the width is characterized by a similar ratio $R = W_2/W_1$, where W_2 is the width after elongation, and W_1 is the width before elongation. Fig. 9 shows relative width of an isoprene rubber plotted against the tensile strain, ε. Elongation leads to a reduction in the width. The ratio $R = W_2/W_1$ in Fig. 9 was used to plot Fig. 10. Fig. 10 shows the wavelength, λ, plotted against the ratio R both for tension (circles) and shrinkage (diamonds). The wavelength during tension and shrinkage is described by a single best fit straight line. The straight line passes close to the origin, and hence the wavelength λ may be described by the equation:

$$\lambda = R\lambda_0 \tag{1}$$

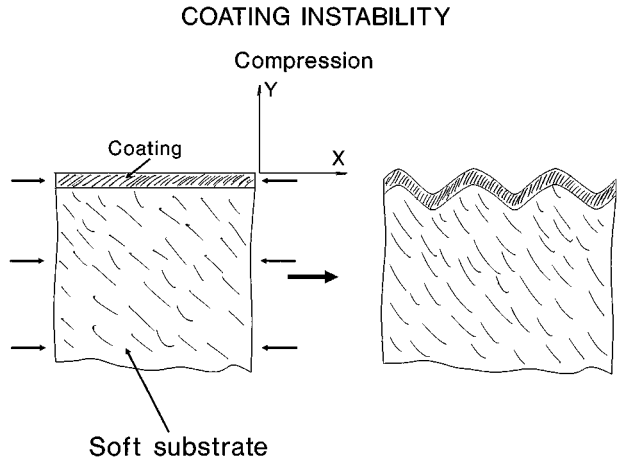

Figure 6 Schematic drawing illustrating appearance of surface wave on an initially smooth surface.

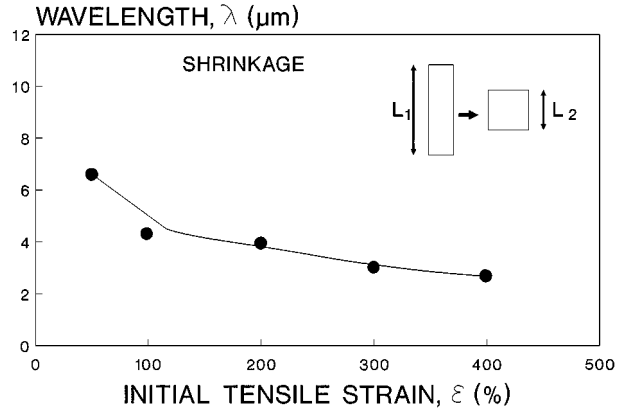

Figure 7 The length of the wave after shrinkage, λ, plotted against the tensile strain, ε, at which the isoprene rubber was coated by a platinum film.

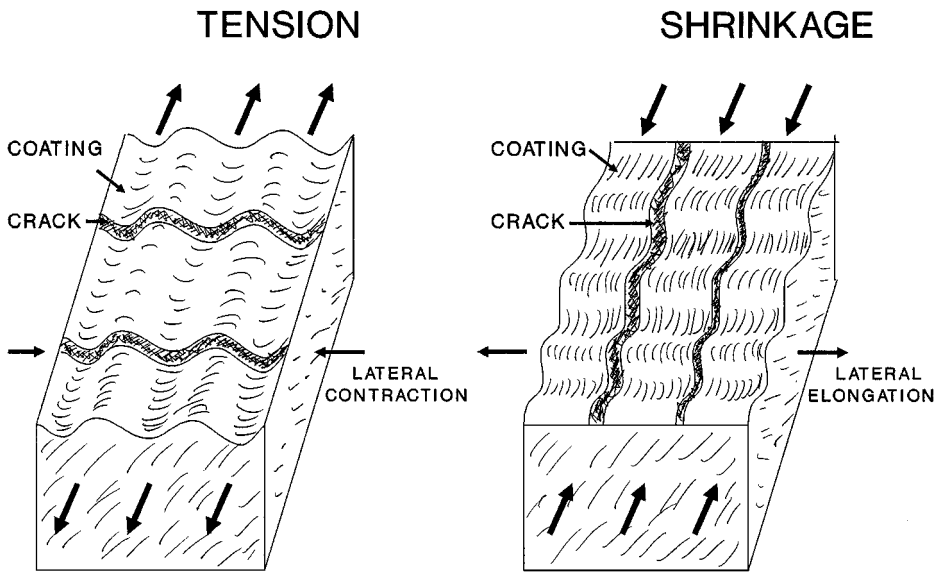

Figure 5 Schematic drawing illustrating surface patterns in tension and after shrinkage.

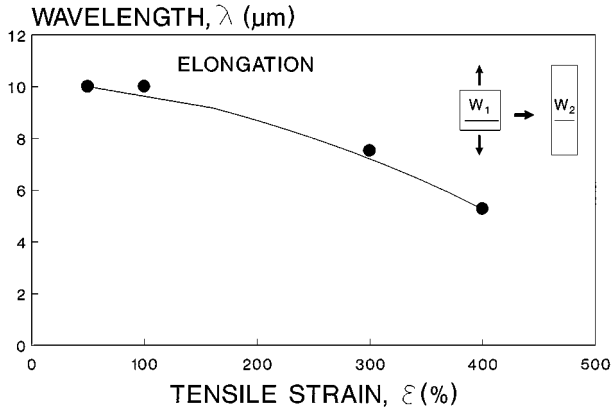

Figure 8 The wavelength, λ, plotted against the tensile strain, ε, for isoprene rubber coated by a platinum film.

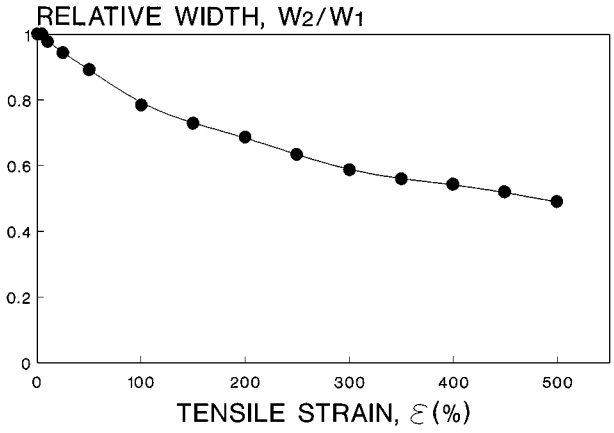

Figure 9 The relative width of an isoprene rubber, W_2/W_1, plotted against tensile strain, ε.

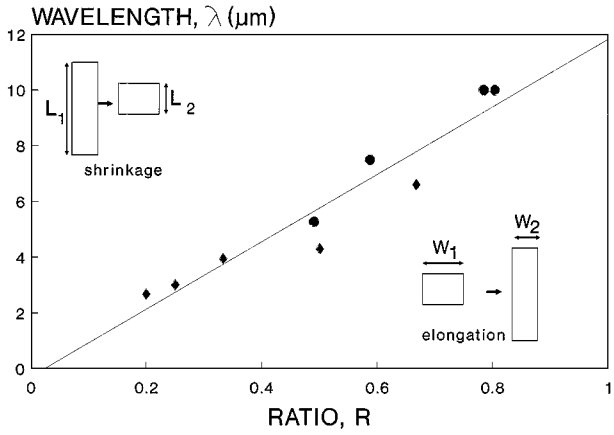

Figure 10 The wavelength, λ, plotted against the ratio of sizes, R, for isoprene rubber coated by a platinum film. $R = L_2/L_1$ after shrinkage and $R = W_2/W_1$ at elongation. The thickness of the platinum layer was constant and equal to 3.8 nm.

where λ_0 is the wavelength corresponding to $R = 1$. Hence, reduction of the wavelength λ in Figs 7 and 8 is caused by the change of the specimen size at deformation.

3.5. Onset of folding with PET substrate

In contrast to the rubber, with the PET substrate folding of the coating is not a critical phenomenon. Fig. 11 shows an SEM micrograph of the PET/Pt elongated to 5% strain at 90 °C. Folding of the coating is not uniform. Large areas are not folded and remain plane. The folded areas appear locally near the cracks. Further elongation leads to merging of the folded areas and formation of uniform folding as in Fig. 1.

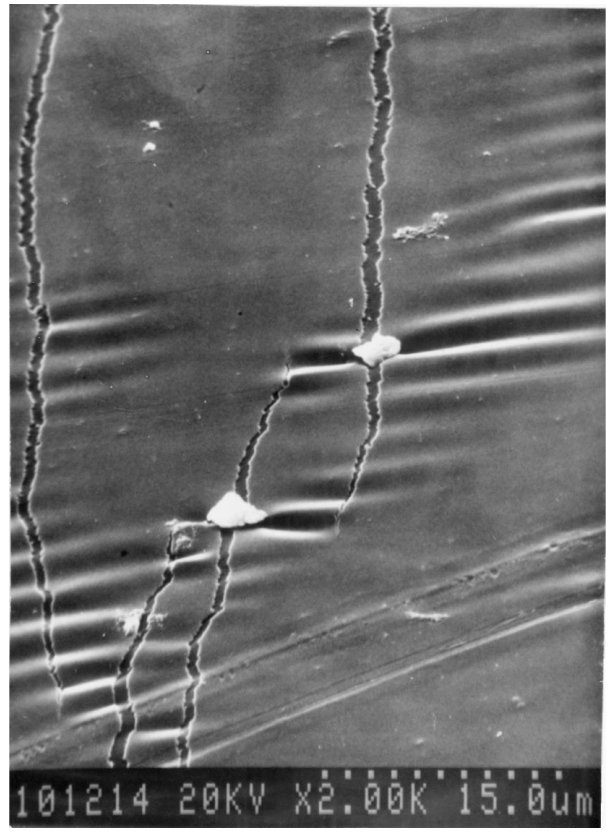

Figure 11 SEM micrograph of the PET/Pt elongated to 5% strain at 90 °C.

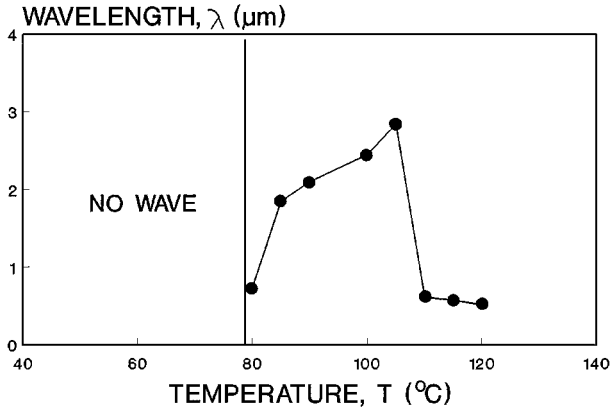

Figure 12 The wavelength, λ, plotted against temperature of elongation, T, for PET/Pt.

Fig. 12 shows the wavelength (period of foldings), λ, plotted against temperature of tension for PET/Pt. The wave did not appear if the temperature was lower than 75–80 °C, the glass transition temperature T_g of PET. The reason why the surface is plane at these temperatures is not clear. At higher temperatures the wave appears, and the wavelength depends on temperature. At $T = 105$ °C a maximum in Fig. 12 is observed.

Fig. 13 shows the storage (Young's) modulus, E', of PET plotted against temperature T. On the curve four different regions may be distinguished. These regions

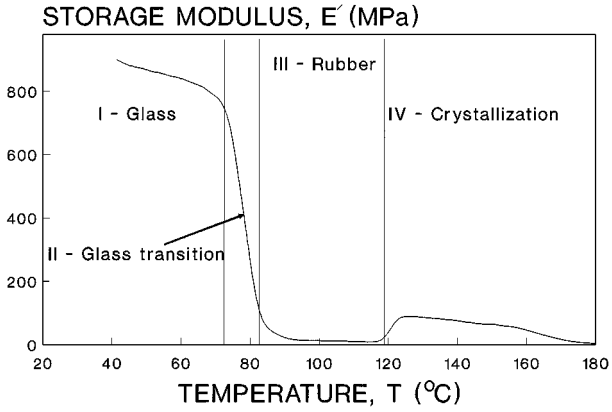

Figure 13 Elasticity storage modulus, E', of PET plotted against temperature T.

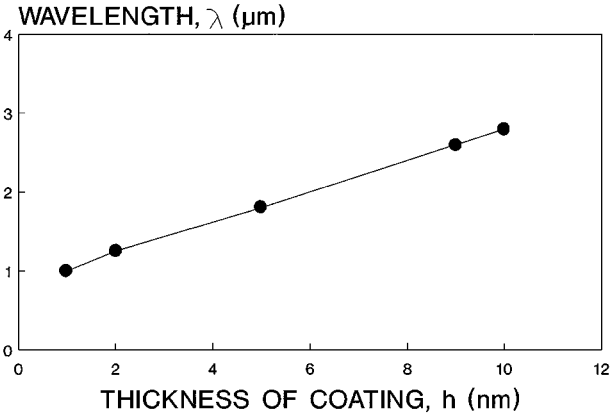

Figure 14 Wavelength, λ, for PET/Pt plotted against the thickness of platinum coating, h.

are related to two temperature transitions in the polymer state. The first transition, from the rigid glassy state (I in Fig. 13) to the soft rubber-like state (III), is observed at 75–80 °C. This, so called glass transition, leads to a dramatic drop in the Young's modulus. The second transition, at 115–120 °C, is crystallization of initially amorphous PET which leads to a significant increase in E'. It is worth mentioning that for polymers this transition is quite unusual.

Comparison of Figs 12 and 13 shows that variation of the wavelength is related to the change of the Young's modulus of the substrate. A decrease in the substrate rigidity leads to an increase in the wavelength.

Fig. 14 shows the wavelength, λ, for PET/Pt plotted against the thickness of the platinum coating, h. The wavelength λ increases almost linearly with the thickness of the coating film.

4. Discussion

The folding of the coating is related to its compression. Features of folding are different in rubber-based and PET-based composites. First, with PET substrates the folding appears near the cracks in the coating. Second, with PET substrates the folding of the coating is not a critical phenomenon. The folded areas appear and grow in comparatively broad intervals of strain. This leads to the assumption that the mechanism of folding is different in these composites. With the rubber substrate the folding appears suddenly on the entire surface of a specimen. This indicates that the folding is caused by elastic buckling instability of the coating under compressive force. The mechanism of folding in PET-based composites is not so clear. The problem of mechanical stability of an elastic coating on a rubber substrate is analyzed in the following section.

4.1. Theory

Mechanical buckling instability of an elastic layer embedded in an elastic medium was considered by Biot [17–19]. Here the stability of a surface layer is considered following his papers. The phenomenon is analyzed using a logic similar to that introduced by Euler to describe the mechanical instability of a rod under compressive force. The upper surface of the coating is free, and its lower surface is adhered to the half-space as illustrated by Fig. 6. The coordinate system is defined so that the Y axis is perpendicular to the coating plane $y = 0$. Compressive force is applied to the elastic layer along the X axis. The shear stresses between the substrate and the coating are neglected. Bending of an elastic layer on an elastic foundation is described by equation [14]:

$$\frac{E_1 I}{1-\nu_1^2}\frac{d^4y}{dx^4} + F\frac{d^2y}{dx^2} + ky = 0 \qquad (2)$$

where E_1 is the Young's modulus, $I = wh^3/12$ is the second moment of area of the layer cross section about the axis of bending, ν_1 is the Poisson's coefficient, h is the thickness, w is the width, and y is the displacement of the coating, F is the longitudinal compressive force in the coating. The effect of the underlying half-space is represented by a lateral load ky acting on the coating. According to Biot, the Winkler's modulus of half-space, k, is [17]

$$k = \frac{Ew}{1-\nu^2}\frac{\pi}{\lambda} \qquad (3)$$

where E is the Young's modulus, ν is the Poisson's coefficient of the substrate, and λ is the buckling wavelength. Equation 3 is valid for sinusoidal deflection of the coating

$$y = A\sin\frac{2\pi x}{\lambda} \qquad (4)$$

The compressive force in the coating, F, is found by substituting Equations 3 and 4 into Equation 2

$$F = E_1 I\left(\frac{4\pi^2}{(1-\nu_1^2)\lambda^2} + \frac{Ew}{4\pi(1-\nu^2)E_1 I}\lambda\right) \qquad (5)$$

The function $F(\lambda)$ is higher than zero at any λ. $F(\lambda)$ has a minimum at some wavelength. If the load in the coating, F, is lower than the minimum F^*, the coating is stable. In contrast, if the load is higher than F^*, the coating is unstable and folds. At the minimum, the

derivative $dF/d\lambda$ is equal to zero. Differentiation gives the expression for the critical wavelength

$$\lambda = 2\pi h \sqrt[3]{\frac{(1-\nu^2)E_1}{3(1-\nu_1^2)E}} \tag{6}$$

This equation predicts the direct proportionality between the wavelength λ and the thickness of the coating, and an increase in λ with the decrease in substrate rigidity.

The critical buckling stress in the coating, $\sigma = F^*/hw$, is:

$$\sigma = \sqrt[3]{\frac{9E_1E^2}{64(1-\nu_1^2)(1-\nu^2)^2}} \tag{7}$$

Neglecting the Poisson's coefficients, the buckling strain is

$$\varepsilon = \sqrt[3]{\frac{9E^2}{64E_1^2}} \tag{8}$$

4.2. Comparison with theory

The folding of an initially smooth coating is explained by the instability of the coating under compressive force. To verify Equation 6 quantitatively, natural rubber was coated with a platinum film, 42 nm in thickness, and elongated to 7% strain. The strain was low because the critical buckling strain is estimated from Equation 7 as 0.024%, and further elongation could reduce the wavelength. The surface wave, 10 μm in length, was observed on the coating.

To calculate the theoretical wavelength, the Young's moduli of platinum $E_1 = 160$ GPa [20] and rubber $E = 1.1$ MPa, the Poisson's coefficients $\nu_1 = 0.36$ and $\nu = 0.5$ were substituted in Equation 6. The value $\lambda = 9.2$ μm was obtained. The agreement of the experimental wavelength 10 μm with the theoretical estimate is good. This confirms that with a rubber substrate the coating folds due to buckling instability under compression. The critical buckling stress in the coating was calculated with Equation 7 as $\sigma = 38$ MPa. This value is lower than the yield stress of the platinum, 70 MPa [20]. Thus, the folding of the coating on the rubber substrate is a completely elastic instability phenomenon.

In contrast to the rubber, for the PET substrate the theoretical predictions disagree with the experimental data. Particularly, an increase in temperature from 100 to 130 °C leads to an approximately 10-fold growth of the Young's modulus of PET in Fig. 13. According to Equation 6, an approximately 2-fold decrease in the wavelength is expected to correspond to this. However, the decrease in λ in Fig. 12 is ≈5-fold.

To calculate the critical buckling stress for PET/Pt at $T = 100$ °C, $E_1 = 160$ GPa, $E = 13$ MPa, $\nu_1 = 0.36$ and $\nu = 0.5$ were substituted in Equation 7, and $\sigma =$ 198 MPa was obtained. This value is ≈3-fold higher than the yield stress of platinum. Evidently, such a high stress cannot be reached in the coating. Hence, for Pt/PET instability of the coating is related to yielding of the platinum. Thus, the buckling instability of the coating on the PET substrate is not just an elastic instability. This may explain the disagreement with the experiment. Equations 6–8 may be used if the critical buckling stress σ is lower than the yield stress of the coating σ_y.

We can describe two possible mechanisms of folding of the coating in PET-based composites. The first is related to yielding of the coating under compression. Study of stability of isolated metal rod under compression showed that yielding of the rod leads to a decrease of the critical buckling stress [21, 22]. Similarly, for PET-based composites buckling may be initiated by yielding of the metal coatings.

The second possible mechanism of folding may be related also with cracking of the coating. In tension the volume of the substrate remains constant, and its width reduces with strain. The coating is rigid and cracks. Hence, the lateral contraction of the coating is lower than that of the substrate. As a result, the coating is compressed and folded along the lateral direction. This may explain initiation of folding by cracks.

5. Conclusions

1. Tension and shrinkage of a rubber coated with a thin platinum film lead to the appearance of wave-like folding of the coating. The mechanism of the folding is mechanical buckling instability of the coating under compressive force.

2. With PET substrate, folding of the coating is also observed. The mechanism of folding is different from that in rubber-based composites. Folding appears near cracks in the coating.

3. Fragmentation of the coating is observed both during tension and shrinkage of the substrate.

Acknowledgements

The authors are grateful to DuPont aid to education program for the financial support of this work. We would like also to thank Dr. M. S. Arzhakov for measurement of the temperature dependence of storage modulus of PET and Professor L. I. Manevich for stimulating discussion.

References

1. F. FAUPEL, C. H. YANG, S. T. CHEN and P. S. HO, *J. Appl. Phys.* **26** (1989) 1911.
2. N. M. MARTYAK, J. E. MCCASKIE, B. VOODS and W. PLEITH, *J. Mater. Science* **32** (1997) 6069.
3. Y. LETERRIER, J.-A. E. MANSON, in European Conf. on Macromolecular Physics, Morphology and Macromechanics of Polymers, Merseburg, Germany, 27 Sept. 1998, pp. 293, 294.
4. S. BAZHENOV, I. V. CHERNOV, A. L. VOLYNSKII and N. F. BAKEEV, *Doklady Academy of Science* **356** (1997) 199.
5. A. L. VOLYNSKII, S. BAZHENOV, O. V. LEBEDEVA, A. N. OZERIN and N. F. BAKEEV, *Vysokomol. Soedin., Ser. A* **39** (1997) 1827.
6. *Idem., J. Applied Polym. Science*, to be published.
7. Y. LETERRIER, L. BOOGH, J. ANDERSONS, J.-A. E. MANSON, *J. Polym. Science, part B, Physics* **35** (1997) 1449.

8. *Idem., ibid*. **35** (1997) 1463.
9. S. BAZHENOV, I. V. CHERNOV, A. L. VOLYNSKII and N. F. BAKEEV, *Doklady Academy of Science* **356** (1997) 54.
10. A. L. VOLYNSKII, S. BAZHENOV, O. V. LEBEDEVA, I. V. YAMINSKII, A. N. OZERIN and N. F. BAKEEV, *Vysokomol. Soedin., Ser. A* **39** (1997) 1805.
11. T. TANAKA, S.-T. SUN, Y. HIROKAWA, S. KATAYAMA, J. KUSERA, Y. HIROSE and T. AMIYA, *Nature* **325** (1987) 796.
12. S. A. DUBROVSKII, *Doklady Academy of Science* **303** (1988) 1163.
13. B. W. ROSEN and N. F. DOW, in "Fracture" Vol. 7, edited by H. Liebovitz (Academic Press, New York, 1972) p. 612.
14. L. D. LANDAU and E. M. LIFSHITZ, "Elasticity Theory" (Nauka, Moscow, 1965).
15. E. WINKLER, "Lehre von der Elastizitat und Festigkeit" (Prag, 1867) p. 182.
16. S. TIMOSHENKO, "Theory of Elasticity Stability" (McGraw-Hill, New York, 1936).
17. M. A. BIOT, *J. Applied Mechanics* **4** (1937) A1.
18. *Idem.*, "Mechanics of Incremental Deformation" (Wiley, New York, 1965).
19. *Idem., Proc. Roy. Soc. Lond., Ser. A* **242** (1957) 1231, 444.
20. I. S. GRIGORIEV and E. Z. MEILIKHOVA (eds.) "Physical Values" (Energoatom, Moscow, 1991) p. 1230.
21. N. J. HOFF, *J. Appl. Mechanics* **18** (1951) 68.
22. L. M. KACHANOV, "Plasticity Theory" (Nauka, Moscow, 1969).

Received 1 June
and accepted 24 June 1999